

## **High-performance, Durable and Low-Cost Proton Exchange Membrane Electrolyser with Stainless Steel Components**

S. Stiber<sup>1</sup>, N. Sata<sup>1</sup>, T. Morawietz<sup>1</sup>, S. A. Ansar<sup>1</sup>, T. Jahnke<sup>4</sup>, J. K. Lee<sup>3</sup>, A. Bazylak<sup>3</sup>, A. Fallisch<sup>2</sup>, A. S. Gago<sup>1,\*</sup>, K. A. Friedrich<sup>1,5</sup>

<sup>1</sup>Institute of Engineering Thermodynamics/Electrochemical Energy Technology, German Aerospace Center (DLR), Pfaffenwaldring 38-40, 70569 Stuttgart, Germany.

<sup>2</sup>Fraunhofer-Institut für Solare Energiesysteme ISE, Heidenhofstraße 2, 79110 Freiburg, Germany.

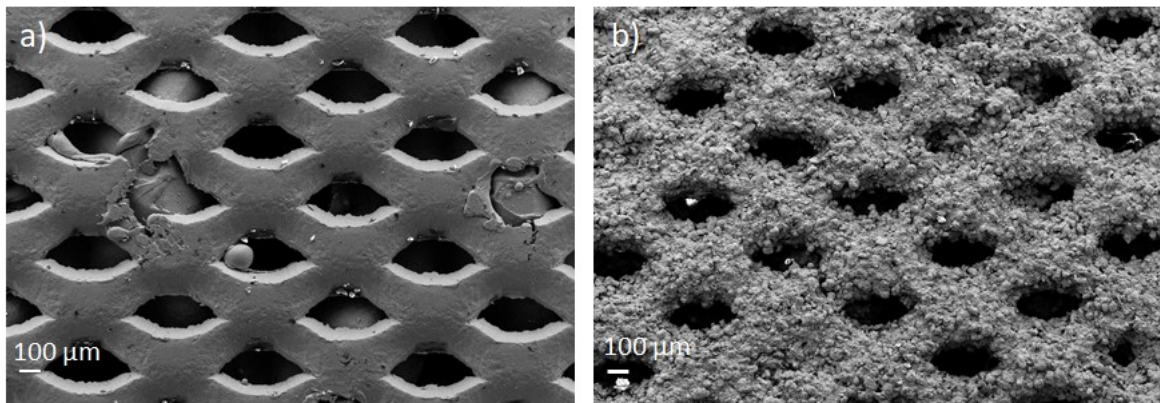
<sup>3</sup>Department of Mechanical and Industrial Engineering, Faculty of Applied Science and Engineering, University of Toronto Institute for Sustainable Energy, University of Toronto, Toronto Ontario, M5S 3G8, Canada.

<sup>4</sup>Institute of Engineering Thermodynamics/Computational Electrochemistry, German Aerospace Center (DLR), Pfaffenwaldring 38-40, 70569 Stuttgart, Germany.

<sup>5</sup> Institute of Building Energetics, Thermal Engineering and Energy Storage (IGTE), University of Stuttgart, Pfaffenwaldring 31, 70569 Stuttgart, Germany.

\*Corresponding author: Tel.: +49 711 6862-8090, Fax: +49 711 6862-747, E-mail address: aldo.gago@dlr.de (A. S. Gago).

1 **1. SEM images of ss-PTL and Nb/Ti/ss-PTL**

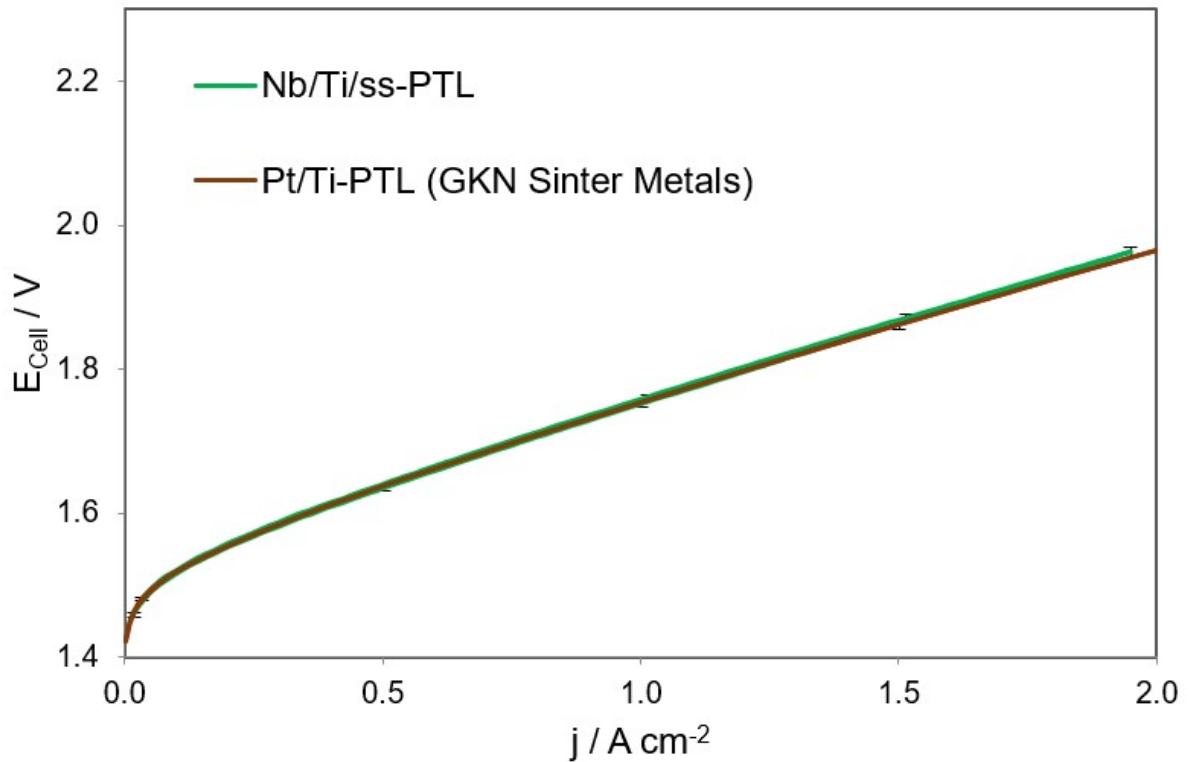


2

3 **Figure S1.** Top view SEM images of a) ss-PTL and b) Nb/Ti/ss-PTL.

4

5 **2. Cell performance comparison with Ti-PTL from GKN Sinter Metals**



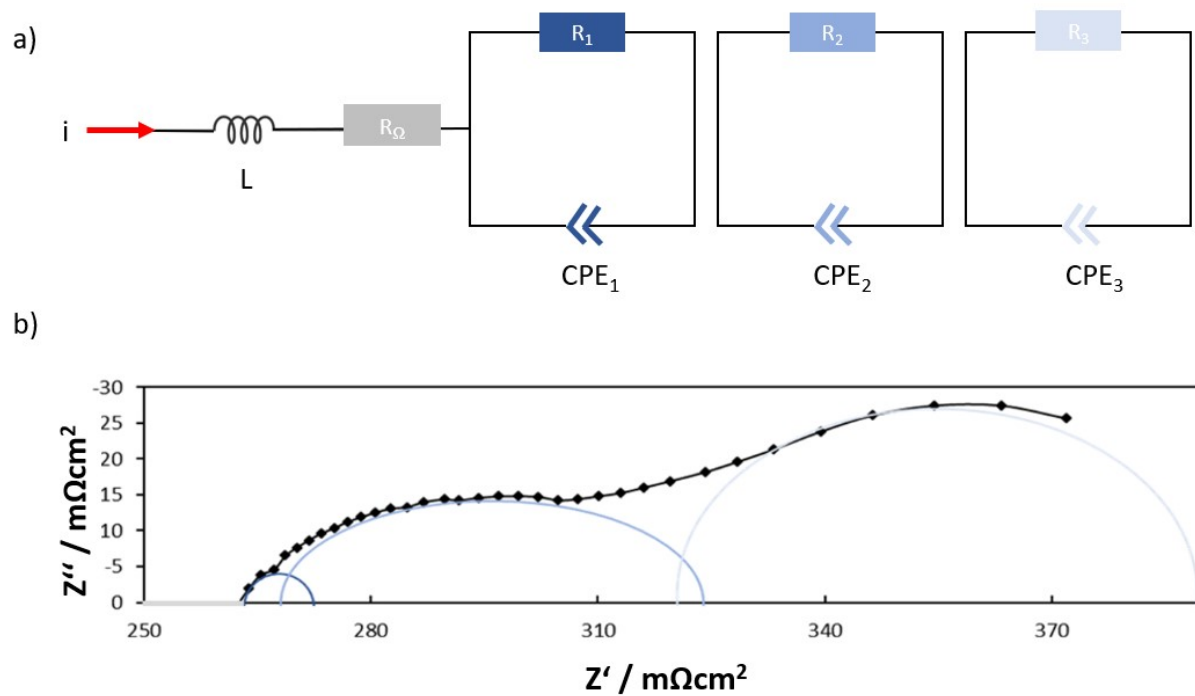
6

7 **Figure S2.** Polarization curves of PEMWE cells with Nb/Ti/ss-PTL compared to Pt/Ti-PTL  
8 (GKN Sinter Metals) at 65 °C.

9

10 **3. Equivalent Circuit for interpretation of EIS data**

11



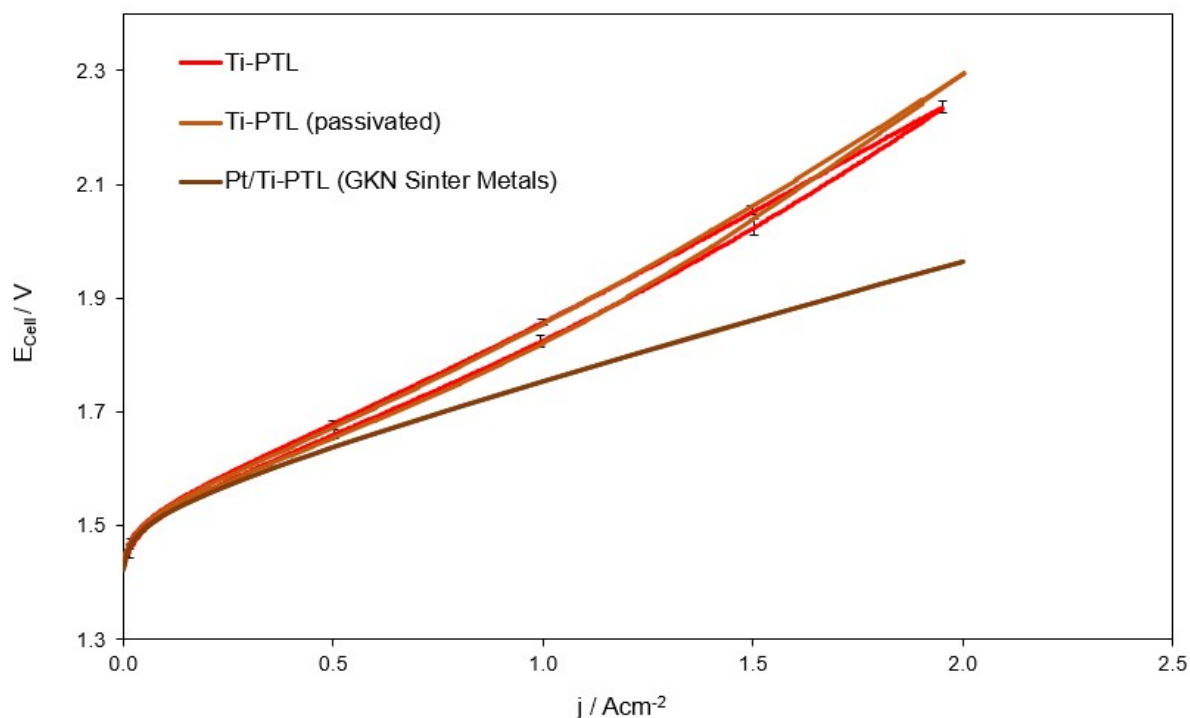
1

2 **Figure S3.** a) Equivalent circuit for analysis of the EIS.  $R_{\Omega}$  corresponds to the ohmic resistance,  
 3 while  $R_1$  can be attributed to hydrogen evolution reaction (HER),<sup>1</sup> charge transfer resistance  
 4 coupled with double layer effects<sup>2</sup> or the first charge transfer of the two-electron process of the  
 5 oxygen evolution reaction (OER).<sup>3</sup>  $R_2$  and  $R_3$  can be related to the charge transfer of the OER  
 6 rate determination step and the mass transport losses<sup>4</sup>, respectively. b) Example of a Nyquist  
 7 plot with the analyzed arcs.

8

#### 9 4. Accelerated Stress Test

10

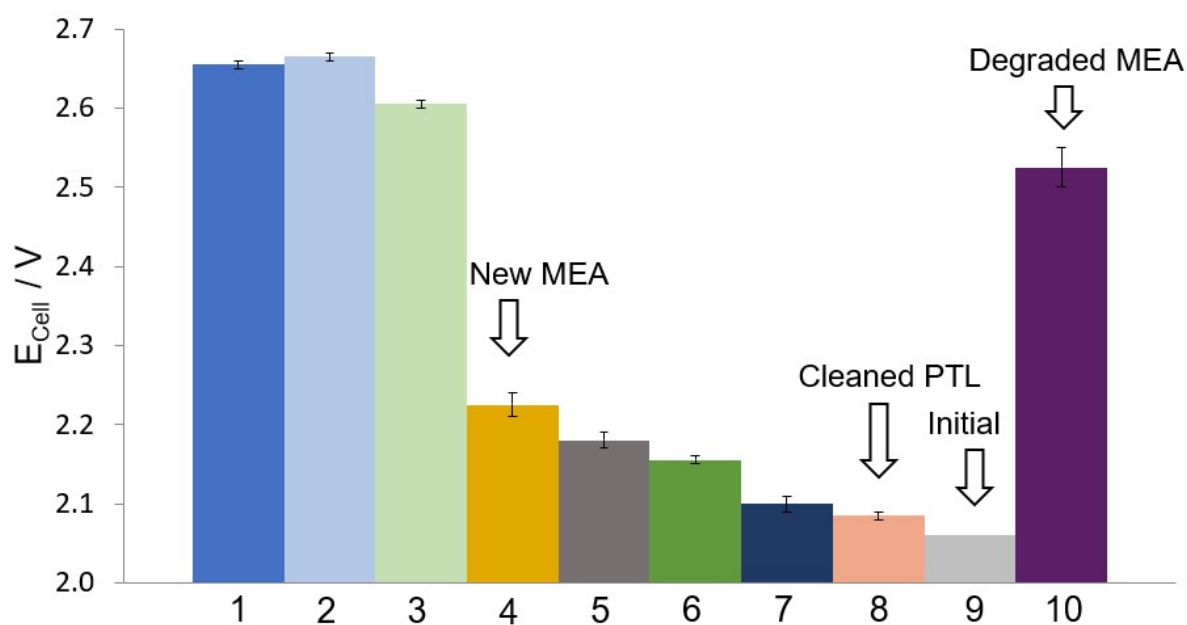


1

2 **Figure S4.** Polarization curves of pristine Ti-PTL, passivated Ti-PTL. To passivate Ti-PTL the  
 3 cell was polarised at constant 2.5 V for about 1 h which was the highest potential reached in  
 4 the durability test performed in Figure 8 of the manuscript, showing that the passivation is not  
 5 the main dominant factor for the low performance at 2 A cm<sup>-2</sup>. The curve of the cell with Pt/Ti-  
 6 PTL (GKN Sinter Metals)<sup>5</sup> is also included for comparison. All tests were measured at 65 °C  
 7 and ambient pressure.

8

## 9 5. Recovery Test



10

1 **Figure S5.** The plot shows the cell potential of Nb/Ti/ss-PTL at 2 Acm<sup>-2</sup> after 1) End of Test,  
2 2) changing the water, 3) replacing carbon paper for a new one, 4) replacing the MEA for a new  
3 one, 5) removing the oxide layer of the anode BPP, 6) removing the oxide layer on the cathode  
4 BPP, 7) cleaning the cathode PTL, 8) cleaning the anode PTL, 8) Beginning of Test, and 9)  
5 using an aged MEA again.

6

7 Figure S5 shows the  $E_{\text{Cell}}$  value at 2 Acm<sup>-2</sup> for each re-assembly step in which the performance  
8 was gradually recovered.

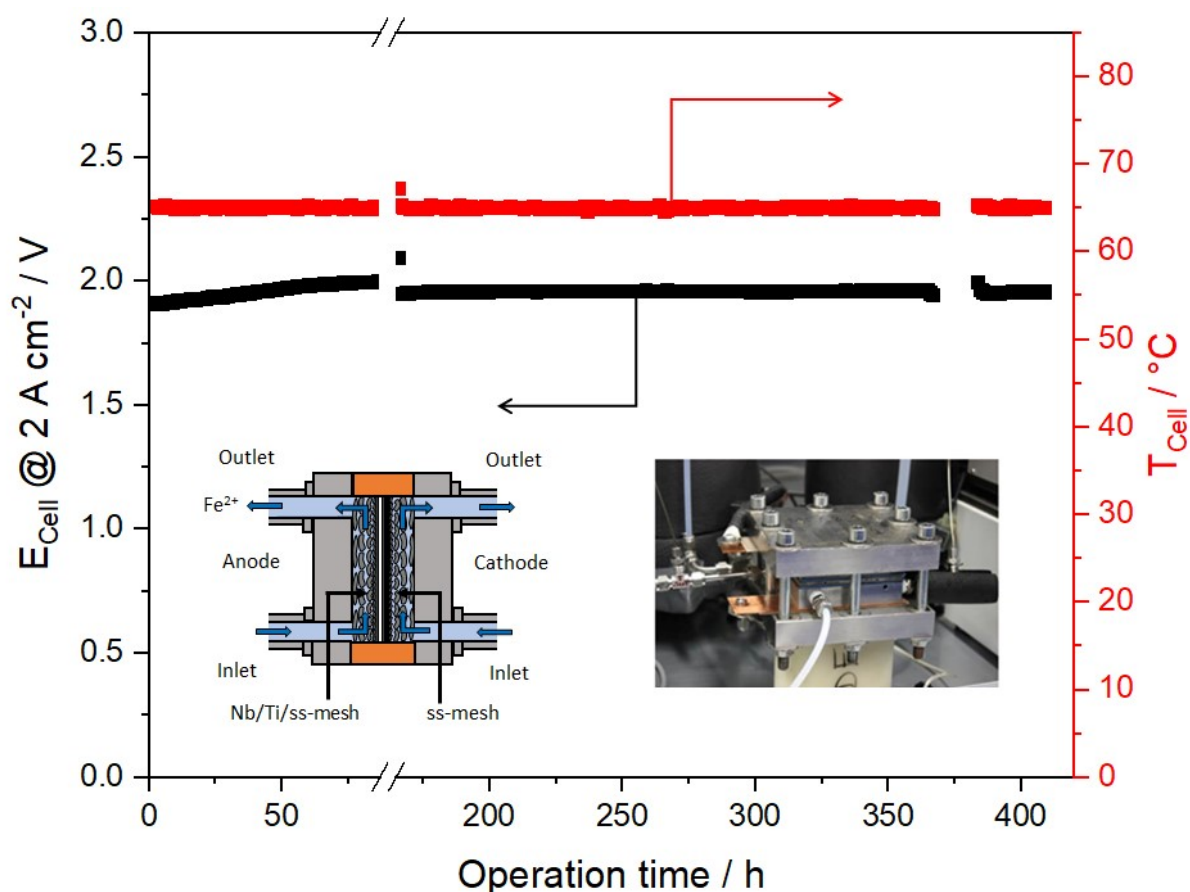
9

- 10 1. Cell performance at the EoT.
- 11 2. Contaminated water was completely replaced by DI water.
- 12 3. The carbon paper was replaced at the interface between the Pt-based cathode and the  
13 uncoated ss-PTL in the cathode.
- 14 4. The MEA was replaced with a new one.
- 15 5. TiO<sub>x</sub> that formed on the Ti/ss-BPP was removed by sanding.
- 16 6. The surface of the ss-BPP on the cathode side was also sanded.
- 17 7. The ss-PTL at the cathode side was cleaned in an ultrasonic bath with several iterations  
18 of DI water and isopropanol, as described in Section 2.2.3.
- 19 8. The Nb/Ti/ss-PTL at the anode side was cleaned in an ultrasonic bath with several  
20 iterations of DI water and isopropanol, as described in Section 2.2.3.
- 21 9. The initial performance at the beginning of the test (BoT).
- 22 10. Aged MEA with new carbon paper, cleaned PTLs and sanded BPP.

23 Clearly, from bars 4 and 10 in the inset of Figure 8, major cell recovery is achieved when  
24 replacing the aged MEA with a new MEA. In fact, the degradation of Nb/Ti/ss-PTL only  
25 contributes to 2.5% of the overall cell degradation, meaning less than 15 μV h<sup>-1</sup> under an AST.  
26 Under normal operating conditions, the effect of the degradation of Nb/Ti/ss-PTL should be  
27 negligible.

28

29 **6. Test of a PEMWE cell with a 25 cm<sup>2</sup> active area**

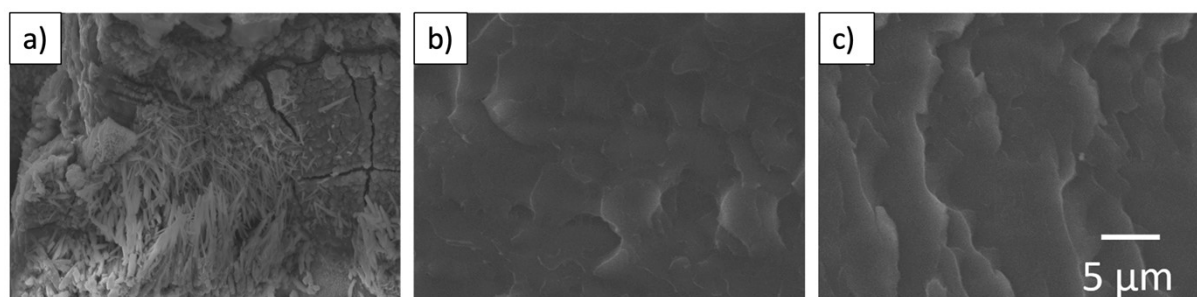


1

2 **Figure S6.** Cell potential ( $E_{\text{cell}}$ ) with respect to operation time of the PEMWE cell with  
 3 Nb/Ti/ss-PTL having a  $25 \text{ cm}^2$  active area at a constant  $2 \text{ A cm}^{-2}$ . The cell temperature is  
 4 indicated on the y-axis. The left image in the inset shows a scheme of the cell with continuous  
 5 water flow on the anode and cathode sides, as is the case for this test. In contrast, the AST is  
 6 carried out with static flow. The right image shows a photo of the PEMWE cell. Measurements  
 7 were performed at ambient pressure and  $65 \text{ }^\circ\text{C}$ .

8

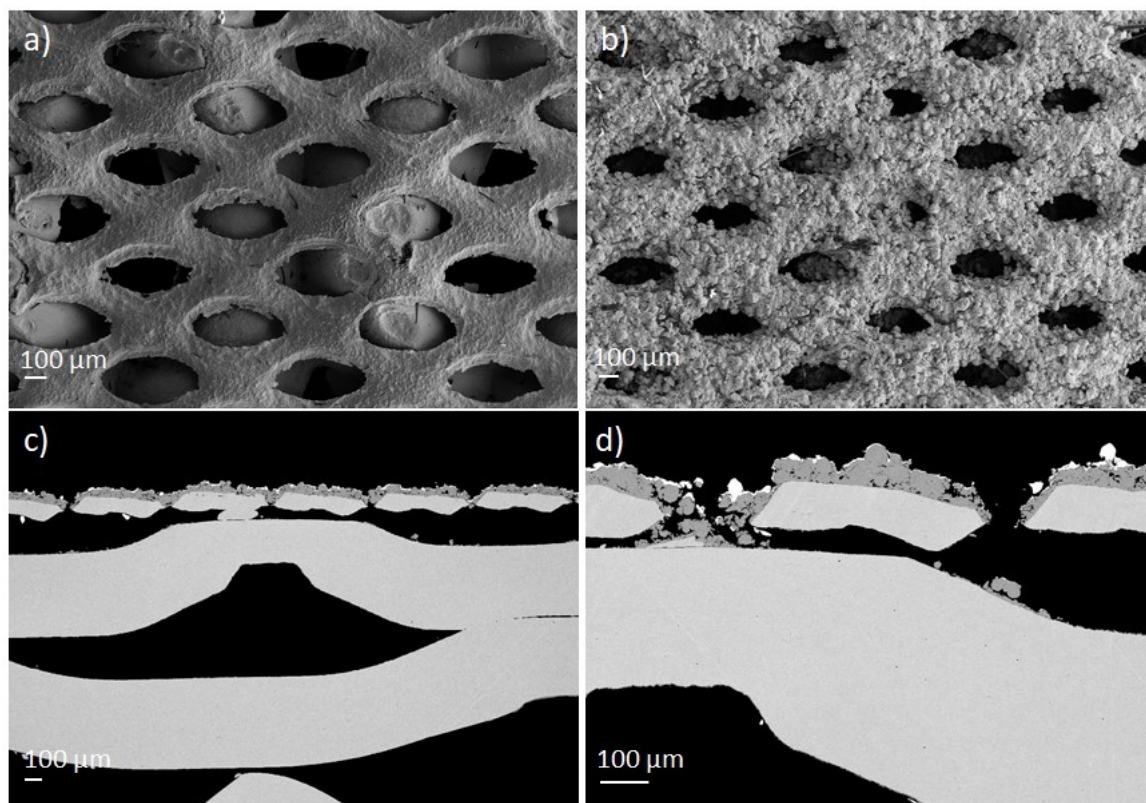
### 9 7. Post-test analysis



10

11 **Figure S7.** SEM images of  $\text{N}_2$ -cleavage of the membrane close to the cathode side, showing  
 12 the possible formation of  $\text{Fe}_3\text{O}_4$  crystals<sup>6</sup> when using a) ss-PTL. This degradation effect did not  
 13 occur when using b) Nb/Ti/ss-PTL and c) Nb/Ti/Ti-PTL.

14



1

2 **Figure S8.** Top view SEM images of a) ss-PTL and b) Nb/Ti/ss-PTL after the PEMWE tests.

3 ss-PTL after a few minutes of testing in the PEMWE cell shows severe pitting corrosion. In

4 contrast, for Nb/Ti/ss-PTL, after more than 1000 h of testing at  $2 \text{ A cm}^{-2}$ , no apparent

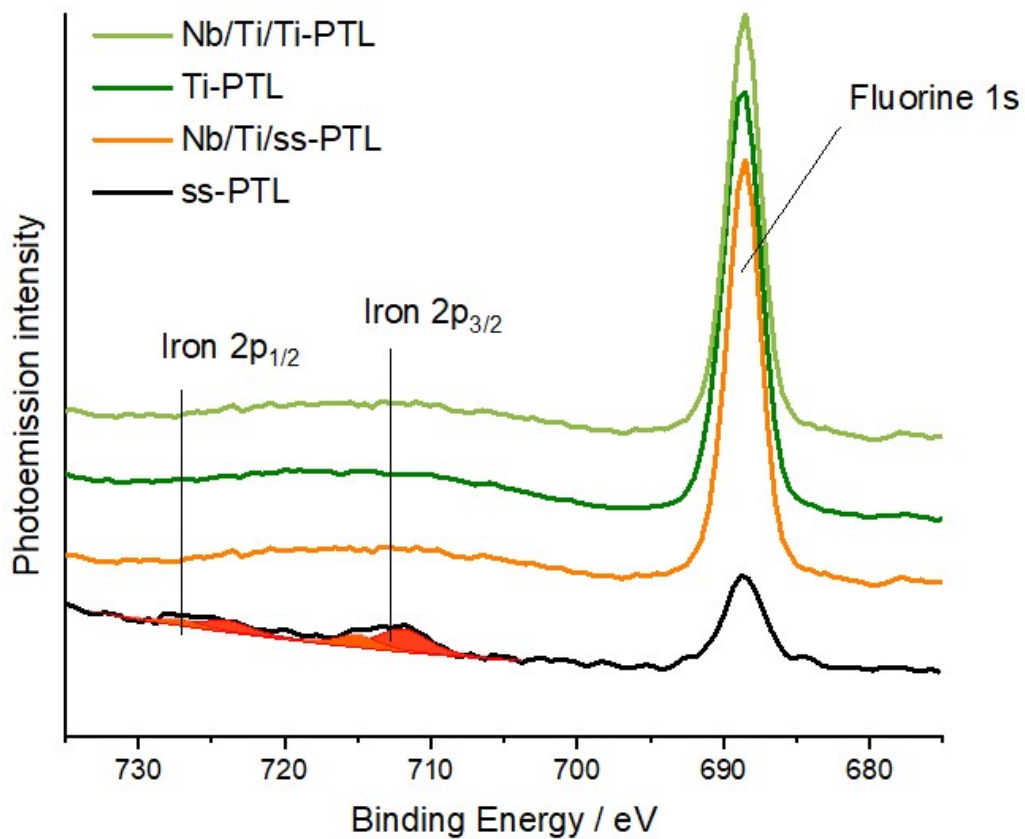
5 degradation, such as surface change, loss of Nb/Ti material, or coating delamination, is

6 observed. Cross-sectional SEM images of Nb/Ti/ss-PTL after operation in the PEMWE cell c)

7 37x and d) 100x magnified. No formation of pin holes on the stainless steel substrate can be

8 observed, confirming the full protection that the Nb/Ti coating can offer against corrosion.

9



1

2 **Figure S9.** X-ray photoelectron emission spectra (XPS) of the cathode surface of the CCMs  
 3 after operation in the AST setup. Detail region for Iron 2p and Fluorine 1s electrons reveal a  
 4 contamination of Iron (mixture of oxide species) of about 1.5 at% on the surface of the cathode  
 5 operated in the PEMWE cell with ss-PTL, while no such contaminant could be observed for  
 6 the cells with Ti-PTL, Nb/Ti/Ti-PTL and Nb/Ti/ss-PTL.

7

## References

1. Siracusano, S., Trocino, S., Briguglio, N., Baglio, V. & Aricó, A.S. Electrochemical Impedance Spectroscopy as a Diagnostic Tool in Polymer Electrolyte Membrane Electrolysis. *Materials*, **11**, 1368 (2018).
2. Lettenmeier, P., Wang, R., Abouatallah, R., Helmly, S., Morawietz, T., Hiesgen, R., Kolb, S., Burggraf, F., Kallo, J., Gago, A.S. & Friedrich, K.A. Durable Membrane Electrode Assemblies for Proton Exchange Membrane Electrolyzer Systems Operating at High Current Densities, *Electrochim. Acta*, **210** 502–511 (2016). <https://doi.org/10.1016/j.electacta.2016.04.164>.
3. Rozain, C., Mayousse, E., Guilleta, N. & Millet, P. Influence of iridium oxide loadings on the performance of PEM water electrolysis cells: Part II – Advanced oxygen electrodes. *Applied Catalysis B: Environmental*, **182**, 123 – 131 (2016).
4. Eikerling, M. & Kornyshev, A.A. Electrochemical impedance of the cathode catalyst layer in polymer electrolyte fuel cells. *Journal Electroanal. Chem.*, **475**, 107-123 (1999).
5. Stiber, S., Balzer, H., Wierhake, A., Wirkert, F. J., Roth, J., Rost, U., Brodmann, M., Lee, J. K., Bazylak, A., Waiblinger, W., Gago, A. S. & Friedrich, K. A. Porous Transport Layers for Proton Exchange Membrane Electrolysis under Extreme Conditions of Current Density, Temperature and Pressure. *Adv. Energy Mater.*, **11**, 2100630 (2021). <https://doi.org/10.1002/aenm.202100630>
6. Mo, J., Steen, S.M., Zhang, F.Y., Toops, T.J., Brady, M.P. & Green, J.B. Electrochemical investigation of stainless steel corrosion in a proton exchange membrane electrolyzer cell. *Int. J. Hydrogen Energy*, **40**, 12506–12511 (2015).